Evaluating Fouling–Resistance and Fouling–Release Performance of Smart Polyurethane Surfaces: An Outlook for Efficient and Environmentally Benign Marine Coatings

6 AUTHORS, INCLUDING:

Vijay Mannari
Eastern Michigan University

39 PUBLICATIONS   **195** CITATIONS

SEE PROFILE

Evaluating Fouling-Resistance and Fouling-Release Performance of Smart Polyurethane Surfaces: An Outlook for Efficient and Environmentally Benign Marine Coatings

Ravi G. Joshi,[1] Achin Goel,[1] Vijay M. Mannari,[1] John A. Finlay,[2] Maureen E. Callow,[2] James A. Callow[2]

[1]Coatings Research Institute, School of Engineering Technology, Eastern Michigan University, Ypsilanti, Michigan 48197
[2]School of Biosciences, University of Birmingham, Edgbaston, Birmingham B15 2TT, United Kingdom

ABSTRACT: Various environmentally friendly approaches have been studied in recent years for effectively controlling biofouling on marine structures. Among these, two distinct and successful approaches are (1) the use of hydrophilic surfaces that control biofouling by resisting the adhesion of fouling organisms and (2) the use of hydrophobic elastomeric surfaces that function by facilitating their easy removal. In this study, we attempted to investigate amphiphilic surfaces for their effectiveness in controlling marine biofouling. Polyurethane surfaces containing tethered hydrophilic, hydrophobic, and amphiphilic moieties were designed and synthesized. The wetting behaviors of these surfaces, as a function of the external environment, were studied by dynamic contact angle (DCA) measurements and their morphologies by atomic force microscopy (AFM). The results from DCA measurements and AFM postulate interesting characteristics of the amphiphilic surfaces. Bioassays with the green fouling alga *Ulva* showed that the amphiphilic surfaces had fouling-resistance and fouling-release potential and provide an insight into the scope of the development of smart marine coatings. © 2009 Wiley Periodicals, Inc. J Appl Polym Sci 114: 3693–3703, 2009

Key words: dendrimers; fluoropolymers; polyurethanes; stimuli-sensitive polymers

INTRODUCTION

Marine biofouling, the colonization of microorganisms, plants, and animals on submerged aquatic surfaces of underwater structures, particularly ships' hulls, is commonly known to increase operational and maintenance costs.[1–4] Marine biofouling has been successfully controlled with self-polishing marine coatings that release active compounds, such as organotin and cuprous oxide, that are toxic to the settling stages of fouling organisms,[5] but many compositions have also been found to have negative effects on nontarget aquatic organisms.[2–4,6] Thus, the use of organotin compounds in marine coatings is now prohibited worldwide, and coatings incorporating cuprous oxide and other biocides are under scrutiny because of these environmental concerns.[2–4,7–9] An acute need has, therefore, been generated for major advances in coatings efficacy

and robustness. To decrease the toxic effects on the marine environment is also a significant challenge because of the diverse range of biofouling organisms, associated fouling mechanisms, and environmental conditions worldwide. A requirement also exists to develop effective marine coatings that have either greatly reduced or no toxicity. This need is being driven by extended service requirements and environmental regulations.[3] A great number of innovations in surface chemistry, biocide development, and coating designs are being studied for the development of alternatives to biocidal antifouling coating formulations.[3] A distillation of formulation and design disclosures to date suggests that among the various approaches used to develop ecofriendly marine coatings, those based on controlled surface morphology to enhance self-cleaning or fouling resistance have attracted more attention by researchers.[3,8,10–31]

For the successful development of such marine coatings, it is critical to understand the basic adhesion mechanisms of marine organisms. An extensive literature search[3,32,33] of the current state of the art indicates that because of the diverse adhesion mechanisms of marine organisms[34] and other numerous factors, such as environmental, material surface, and bulk characteristics (chemical and

physical configurations), the range of characteristics of secreted adhesives and their complex interactions with the contacting surface make it difficult to deduce specific adhesion mechanism(s). The literature[3,4,7,17,32–37] reveals that many of the fouling organisms primarily use protein-based adhesives to attach themselves to the contacting surfaces. Previous studies and experimental data revealed in the earlier literature have claimed that hydrophilic surfaces, such as poly(ethylene oxide) and poly(ethylene glycol) (PEG; commonly used in drug delivery, biomedical, and pharmaceutical applications), because of their low protein adsorption, good stability, and low toxicity, are more resistant to the adhesion (attachment) of marine organisms.[3,8,17,21,26,27,35–39] Hydrophobic surfaces, for example, silicone- and fluorine-based elastomers, are commonly used as marine fouling-release coatings because of their low surface energy and interesting mechanical properties.[3,13,15–17,26,31,35–37,39–41] Commercial fouling-release coatings based on silicone elastomers "release" accumulated biofouling either through the action of hydrodynamic forces generated as a vessel moves through water or through direct cleaning by hand or with robots and have been researched widely.[3,8,22,40,41] However, this generation of fouling-release coatings based on siloxane elastomers have a number of shortcomings and are unsuitable for use on the majority of vessels.[3,8,22,40,41] From the previous discussion, one can infer that an amphiphilic surface that combines both hydrophobic and hydrophilic mechanisms would provide an effective and environmentally benign solution to fouling control by discouraging the hydrophobic or hydrophilic interactions of fouling organisms and thus result into their weak adhesion and/or easy removal.

In this study, we designed and developed polyurethane (PU) materials using flexible dendritic polyol with tethered amphiphilic moieties. The surfaces of such polymeric assemblies are expected to show interesting characteristics in different contact environments, such as in air and in water. The choice of a PU backbone provided superior mechanical properties, including a high modulus and toughness, compared to the currently used siloxane elastomers, which have a low modulus and are susceptible to damage.[3,8,16,22,35–37,39–41]

The surfaces were evaluated with the green alga *Ulva*, which is the most common macroalga that fouls ships and other marine structures. The dispersal of *Ulva* is mainly through motile, quadriflagellate zoospores (ca. 7–8 μm in length), which swim in the water until they locate a surface on which to settle.[42] The number of spores that settle (attach) provides an indication of the potential antifouling properties of surfaces. The settled spores rapidly germinate into sporelings (young plants), which adhere weakly to fouling-release coatings.[43,44]

Ulva spore settlement and sporeling strength of attachment assays were conducted on PU surfaces prepared with (1) tethered hydrophilic [poly(ethylene oxide) chain] moieties, (2) tethered hydrophobic (perfluoroalkyl chain) moieties, and (3) tethered amphiphilic chains containing both hydrophobic and hydrophilic moieties. These studies postulate potential characteristics of the amphiphilic surfaces and provide an insight into their scope for the development of smart marine coatings with dual (fouling-resistance and fouling-release) properties.

EXPERIMENTAL

Materials and methods

The materials used in this study with their sources were as follows:

- Boltorn H2004 (dendritic polyol polymer, certified) from Perstorp Specialty Chemicals (Perstorp, Sweden).
- Isophorone diisocyanate (IPDI; 98%, Aldrich Chemicals, St. Louis, MO).
- Dibutyl tin dilaurate (95%, Aldrich).
- Methoxy-terminated poly(ethylene glycol) (MPEG; weight-average molecular weight = 750 g/mol, Clariant Specialty Chemicals, North America Region, Charlotte, NC).
- 1H,1H,2H,2H-Perfluorooctanol (PFO; 97%, Alfa Aesar, Ward Hill, MA).
- The ethoxylated fluoroalkyl surfactant Zonyl FSO-100 (Sigma–Aldrich).
- Tetrahydrofuran (anhydrous 99% inhibitor free, Aldrich).
- Acrylic polyol (Joncryl 920, Johnson Polymers, part of BASF polymers, Florham Park, NJ).
- Petroleum ether (anhydrous, Aldrich).
- Plain glass microscope slides (75 × 25 mm^2, Fisher Scientific, Pittsburg, PA).
- ACT phosphated cold-roll steel panels (6 × 4 in.^{2}, ACT Test Panels, Inc., Hillsdale, MI).

All of the reagents and materials were certified and were used without further purification unless otherwise mentioned.

The final products were characterized for Fourier transform infrared (FTIR) spectroscopy and NCO content (%) as per ASTM D 5155-91 test method A. The methods used for surface analysis [contact angle (CA) measurement and micro/nanoroughness] and biological tests are described in the Characterization section of this article.

Synthesis of the IPDI-based prepolymers

NCO-functional prepolymers with predetermined NCO content (%) were synthesized by the reaction
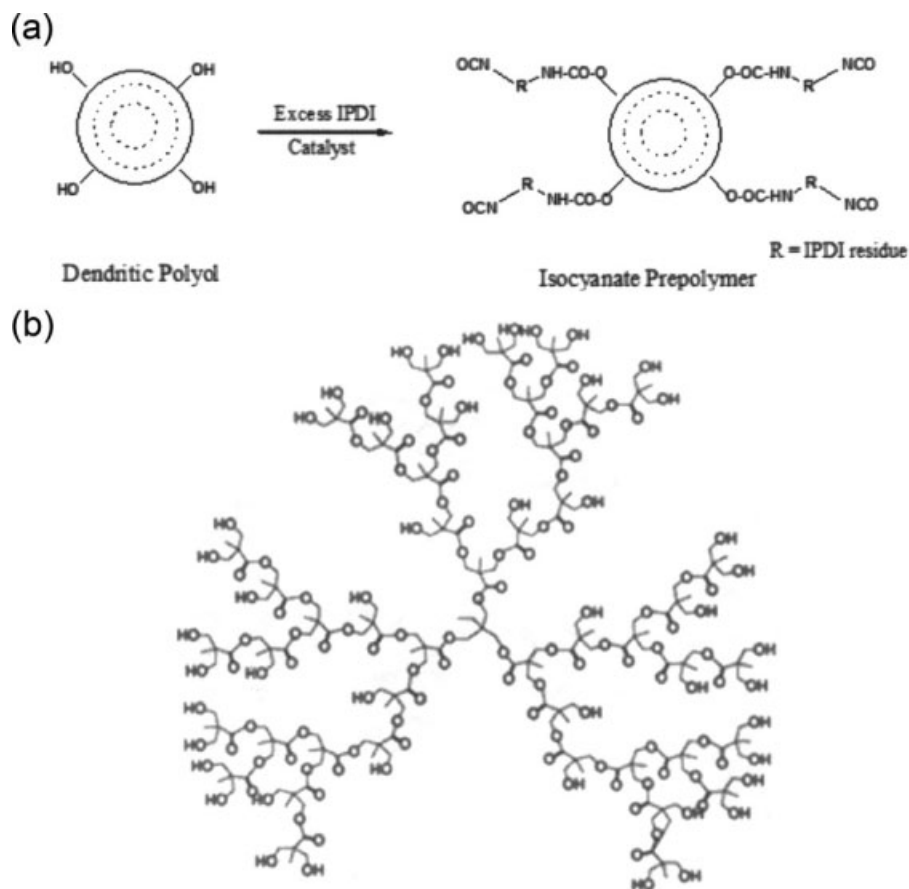
Figure 1 (a) Schematic representation of the preparation of the isocyanate prepolymer and (b) generic structure of the Boltorn H2004 dendritic polyol.[45]

of a molar excess of IPDI with dendritic polyol (Boltorn H2004) with tetrahydrofuran as the solvent [Fig. 1(a)]. The generic structure of Boltorn H2004 dendritic polyol[45] is shown in Figure 1(b). For conditions of this synthesis, the guidelines reported in the literature[24,36,37,46] were followed, and the details are reported elsewhere in the literature.[24,36,37,46] The previous literature also showed that good control of chain extension could be achieved through the use of a large excess of isocyanate or by the addition of dibutyl tin dilaurate as a catalyst.[24,36,37,46] Also, in addition to the monofunctional compound (predominant product), other compounds (difunctional and trifunctional) were also present in the product.

Functionalization of the prepolymer with amphiphilic side chains, PFO, and PEG

In the second step, the prepolymer was reacted separately with calculated amounts of A: perfluo octanol (PFO), B: methoxy terminated PEG with a molecular weight of 750 g/mol (MPEG), and C: fluoro surfactant FSO-100, with an NCO/OH ratio of 2 : 1 as represented in Figure 2. These reactions were carried out for 6–12 h at 50°C in the presence of a dibutyltin dilaurate catalyst.
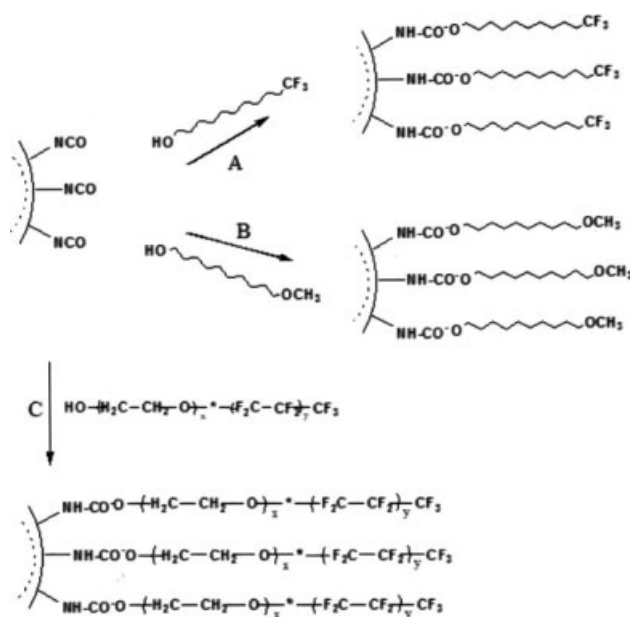
Figure 2 Tethering of the isocyanate-terminated prepolymer with functional moieties A, B, and C.

TABLE I
List of Films

Composition	Sample code for the DCA and AFM measurements	Sample code for the bioassays with the green fouling alga (*Ulva*)
Dendritic polyol, diisocyanate, and acrylic polyol	Control PU	MRC
Dendritic polyol, diisocyanate, hydrophilic (MPEG derivative) compound, and acrylic polyol	MPEG–PU	MRPE
Dendritic polyol, diisocyanate, hydrophobic (PFO derivative) compound, and acrylic polyol	PFO–PU	MRF
Dendritic polyol, diisocyanate, amphiphilic compound, and acrylic polyol	Zonyl FSO-100–PU	MRZ100

Preparation of the films

Joncryl-920 (acrylic polyol) was mixed with tethered —NCO prepolymers in definite proportions. The mixture was applied to the cleaned glass plates and steel panels to yield a dry film thickness of about 25 µm. After 30 min of ambient curing, the samples were cured at 100–120°C for 2 h in an air oven. Control film samples, without any hydrophobic or hydrophilic modifications, were also prepared in an identical manner for comparative study. The resultant coatings are coded as shown in Table I.

A Nicolet 510P FTIR spectrophotometer (Irvine, CA) was used to monitor the urethane formation reaction. The absorption peaks at 1532, 1763, and 3352 cm^{-1} confirmed urethane formation. Also, the lack of appreciable absorption around 2270 cm^{-1} (—NCO) and 3400 cm^{-1} (—OH) was indicative of the quantitative consumption of isocyanate and hydroxyl groups.

Characterization

CA measurements

This procedure was essentially published previously but is included here for completeness.[35–37] A First Ten Angstrom FTA-200 dynamic contact angle (DCA) analyzer (Portsmouth, VA) was used for CA determination. We used two test liquids, water (a hydrophilic liquid capable of forming hydrogen bonds with the substrate) and hexadecane (a nonpolar, oleophilic liquid). Two spots were marked on the film surface roughly 0.5 cm in diameter. One slide was used for CA determination with each test liquid. A 10-µL test liquid (water or hexadecane) droplet was allowed to fall onto the surface at a rate of 1 µL/s within the marked spot. A movie was captured at the rate of 1 frame/s, and the CA reading was noted after 15 s (after we allowed the liquid droplet to equilibrate with the surface). The readings obtained at two different spots for the same test liquid were averaged and reported. Once the CA was determined in air, the samples were immersed in deionized (DI) water for 12 h. The samples were then taken of the water, and the excess water was wiped off. The CAs on these surfaces were then instantaneously determined with the same test liquids in the same spot to minimize the error due to heterogeneity of the surface. After the CA of the wet surfaces was determined, these surfaces were dried at ambient temperature for at least 12 h, and the CA was measured again to study the change in wetting behavior of the surfaces (postdrying stage).

Atomic force microscopy (AFM) roughness measurements

Sample preparation. Liquid coatings were applied on 1 × 1 cm^2 phosphated mild steel panels to achieve a dry film thickness of 25 µm. The samples were cured as described in the Experimental section. For AFM imaging, the edges of the samples were sealed with marine epoxy to avoid permeation of water during the immersion in water. The samples were first fixed firmly to the AFM mounting disk with ethyl cyanoacrylate adhesive.

Procedure. This procedure was essentially published previously but is included here for completeness.[35–37] The samples were imaged with a Digital Instruments (Plainview, NY) multimode atomic force microscope with a NanoScope 3a controller and an E-scanner (X–Y scanning limit = 15 µm, Z limit = 2 µm) in the tapping mode. Both height and phase were captured at an image size of 5 × 5 µm^2. Each sample was thus imaged under three different conditions:

1. Prescan: The samples were imaged dry without any treatment other than mounting.
2. Wet: The samples were imaged in DI water after soaking in DI water for at least 12 h and not more than 24 h.

3. Postscan: The samples were again imaged after they were allowed to dry for at least 12 h.

Two sets of images were captured for each sample under each of the conditions. Each captured image was flattened with a binomial flattening algorithm (a best-fit second degree polynomial was subtracted from each scan line). This allows for correction of to correct error in the image introduced by hysteresis in the piezoelectric scanner. Roughness data was then calculated from each of the flattened images, and an average of the roughness data was also calculated. In the present study, we used root mean square (rms) roughness – average of height deviations taken from the mean data plot.

Ulva assays

Zoospore settlement. The coated slides (three per treatment) were incubated with a suspension of zoospores (1×10^6/mL) for 1 h in darkness at 20° as described in Callow et al.[42] The slides were washed in seawater to remove unsettled (swimming) spores and fixed with 2.5% glutaraldehyde in seawater. The density of zoospores attached to the surface was counted on each of three replicate slides with an image analysis system attached to a fluorescent microscope. Spores were visualized by the autofluorescence of chlorophyll. Counts were made for 30 fields of view (each 0.17 mm^2) on each of the three replicate slides.[43]

Growth and strength of the attachment of the sporelings. The coated slides (five replicates per treatment) were incubated with 10 mL of a spore suspension as described previously. After they were washed in artificial seawater to remove unsettled (swimming) spores, the slides were returned to the dishes, and 10 mL of growth medium was added.[43] After they were cultured for 7 days, a green lawn of sporelings (young plants) covered the surface of the slides. Growth was estimated by direct measurement of fluorescence from chlorophyll contained within the chloroplasts of the sporelings (young plants) with a Tecan plate reader (GENios Plus, Mannedorf/Zurich, Switzerland). Fluorescence was recorded as relative fluorescence units (RFU) from direct reading.[47] The strength of attachment of the sporelings was determined by jet washing at a range of impact pressures (one slide per pressure) with the water jet described by Finlay et al.[48] RFU readings (70 per slide) were taken from the central part of the slide that was exposed to the water jet. The percentage removal was calculated from the difference in fluorescence readings before and after exposure to the water jet. A single slide was exposed to each water pressure, and the percentage removal values were plotted to produce a curve of removal as a function of water pressure. From the curve, the water pressure required to remove 50% of the *Ulva* sporeling biomass from each type of surface was determined. Comparison of these values allowed the surfaces to be ranked according to fouling-release performance.

In addition to the urethane samples, glass and the polydimethylsiloxane (PDMS) Silastic-T2 (Dow Corning, Midland, MI) were incorporated into the study to act as nonrelease and foul-release surfaces, respectively.

RESULTS AND DISCUSSION

Design and synthesis of smart PU surfaces

The synthesis of the IPDI-based prepolymer and its functionalization with different active compounds were carried out with guidelines for the optimal conditions for similar reactions reported in the literature.[36,37,46] The formation of the intermediate and final products were confirmed by the percentage NCO contents of the products and by the fact that this reaction was monitored by FTIR spectroscopy with the disappearance of the absorption peak corresponding to the —OH group ($\sim$3400 cm^{-1}).

One of the critical requirements in the designing such *smart* surfaces is to have a very flexible polymer backbone that facilitates "switching" of tethered moieties, in response to external stimuli.[49] The PU networks were built with dendritic polyol, IPDI, hydroxyl functional acrylic polyol, and different functional moieties [Figs. 1(a) and 2]. For the functionalization of prepolymer (as described in Fig. 2), dendritic polymers substituted by hydroxyl groups are particularly suitable. These dendritic polymers are of a polyester type consisting of a multifunctional core, from which branches extend to give a highly branched inherent structure with a large number of terminal hydroxyl groups. The core consists of a specific polyalcohol. The hyperbranched structure is generally built from 2,2-dimethylol propionic acid.[45] We used Boltorn H2004, a commercially available certified dendritic polyol from Perstorp Specialty Chemicals,[45] which was reported to have six terminal hydroxyl groups, a hydroxyl value of 105–125 mg of KOH/g, an acid value of 7 mg (maximum) of KOH/g, a weight-average molecular weight of 3200 g/mol, a glass-transition temperature of −35°C, and a viscosity of 15 Pa s at 23°C.[45] The generic structure of Boltorn dendritic polyol[45] is shown in Figure 1(b). The dendritic polyol serves as a soft segment and also provides sites for tethering amphiphilic moieties. We believe that such a structure would provide the necessary backbone flexibility and, hence, facilitate orientation (switching) of the tethered structures. Also, it has been reported that small amounts (5 wt %) of an amphiphilic
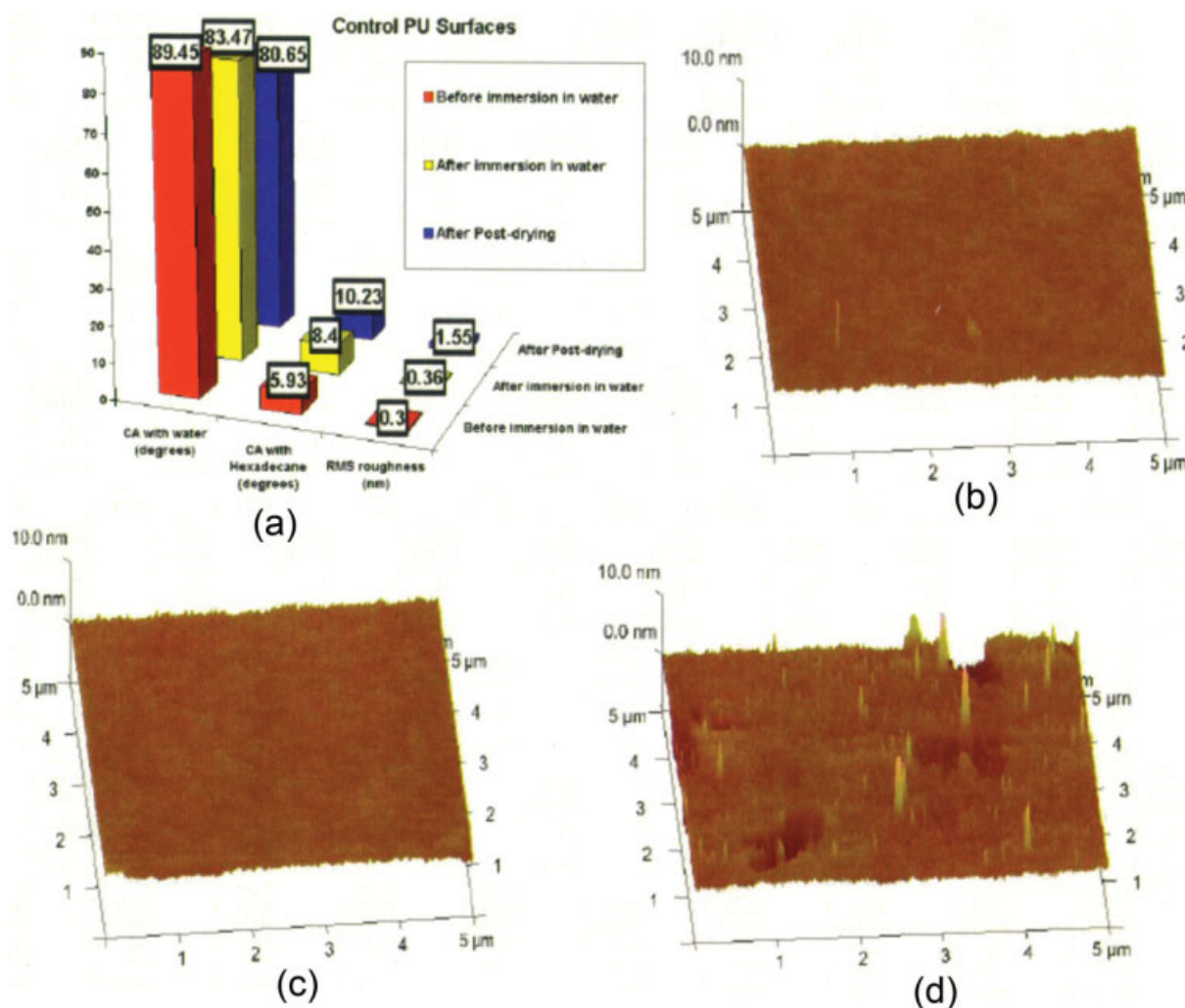
Figure 3 (a) Control PU surfaces (CA and rms roughness), (b) AFM image before water immersion, (c) AFM image after water immersion, and (d) AFM image for postdrying. [Color figure can be viewed in the online issue, which is available at www.interscience.wiley.com.]

moiety is sufficient to give amphiphilic character to the surfaces with unaltered bulk properties.[39,50]

## Corroboration of the DCA and AFM analysis results

The DCA results, in conjunction with the AFM analysis, of the smart PU coatings with different surface modifications gave meaningful information about their wetting behavior and surface topography in different contact environments. The analysis gave promising results and built a strong foundation for our current and future efforts to develop a potential amphiphilic marine coating that can combat the diverse adhesion mechanisms of marine organisms. Here, we explained the water and hexadecane wetting behavior of smart PU coatings by taking rms surface roughness into account. The standard deviation in all of the CA experiments was ±2–3°.

Control PU surfaces

Figure 3(a) shows a graphical representation of the roughness data and CA results with water and hexadecane in three different conditions: before water immersion, immediately after water immersion, and postdrying. The control PU samples were smooth and did not undergo any noticeable change in surface topography after immersion in water. The CA with water and hexadecane and the surface roughness remained nearly constant, which indicated no surface reorganization. The postdrying samples showed increased roughness, which indicated some ordered orientation in air.

Hydrophilic surfaces containing MPEG

Figure 4(a) shows the results for the hydrophilic surfaces under different conditions. The hydrophilic surfaces containing MPEG showed no difference in
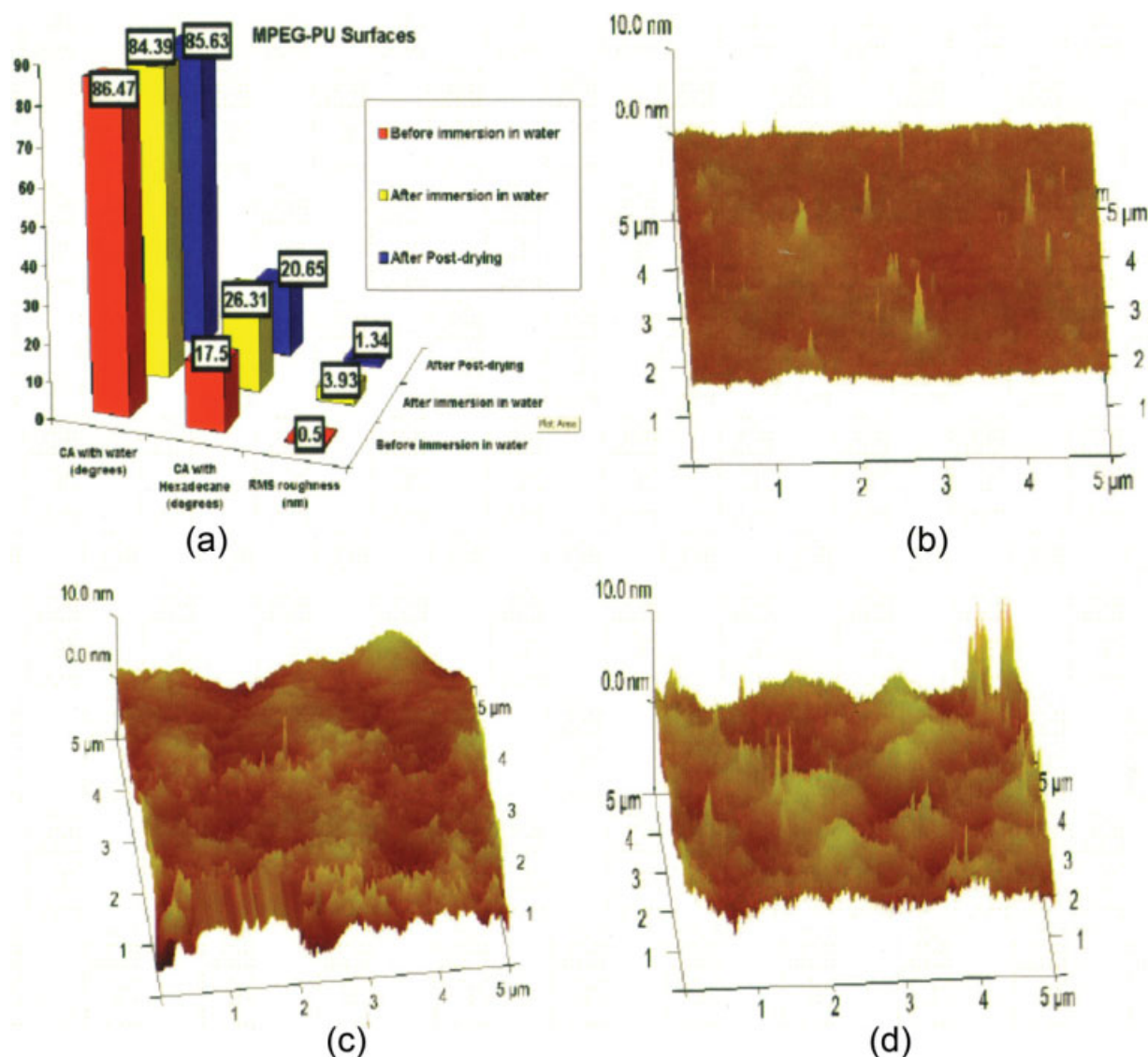
Figure 4 (a) MPEG–PU surfaces (CA and rms roughness), (b) AFM image before water immersion, (c) AFM image after water immersion, and (d) AFM image for postdrying. [Color figure can be viewed in the online issue, which is available at www.interscience.wiley.com.]

water CA after immersion in water and were comparable to the control. However, a higher CA with hexadecane compared to that of the control PU was indicative of the fact that the surface chemical composition of the hydrophilic surfaces was different than that of the control because hexadecane is nonpolar. The increase in the surface roughness with immersion in water from 0.5 to 3.93 nm is believed to be the result of the perpendicular orientation of the MPEG chains [see Fig. 4(c)]. We attributed the higher CA for these surfaces, despite the increase in surface free energy (due to the migration of polar groups at the surface), to the surface roughness, which is known to reduce the effective contact area and, hence, provide a higher CA. For the postdrying samples, the surface roughness decreased; this was probably because of the

collapse of straightened MPEG chains in the hydrophobic air environment.

Hydrophobic surfaces containing PFO

Figure 5(a) shows results of hydrophobic surfaces in different environments. The surface topography [Fig. 5(b)] and roughness results [Fig. 5(a)] indicate the orientation of the hydrophobic PFO chains in air. When these surfaces were immersed in water [Fig. 5(c)], the hydrophobic PFO chains bent toward the hydrophobic PU surface or clustered together, which thereby decreased the rms roughness. Thus, a drop in water CA after immersion in water was attributed entirely to the decrease in surface roughness. After postdrying [Fig. 5(c)], the hydrophobic PFO chains again reoriented perpendicularly to the surface in a
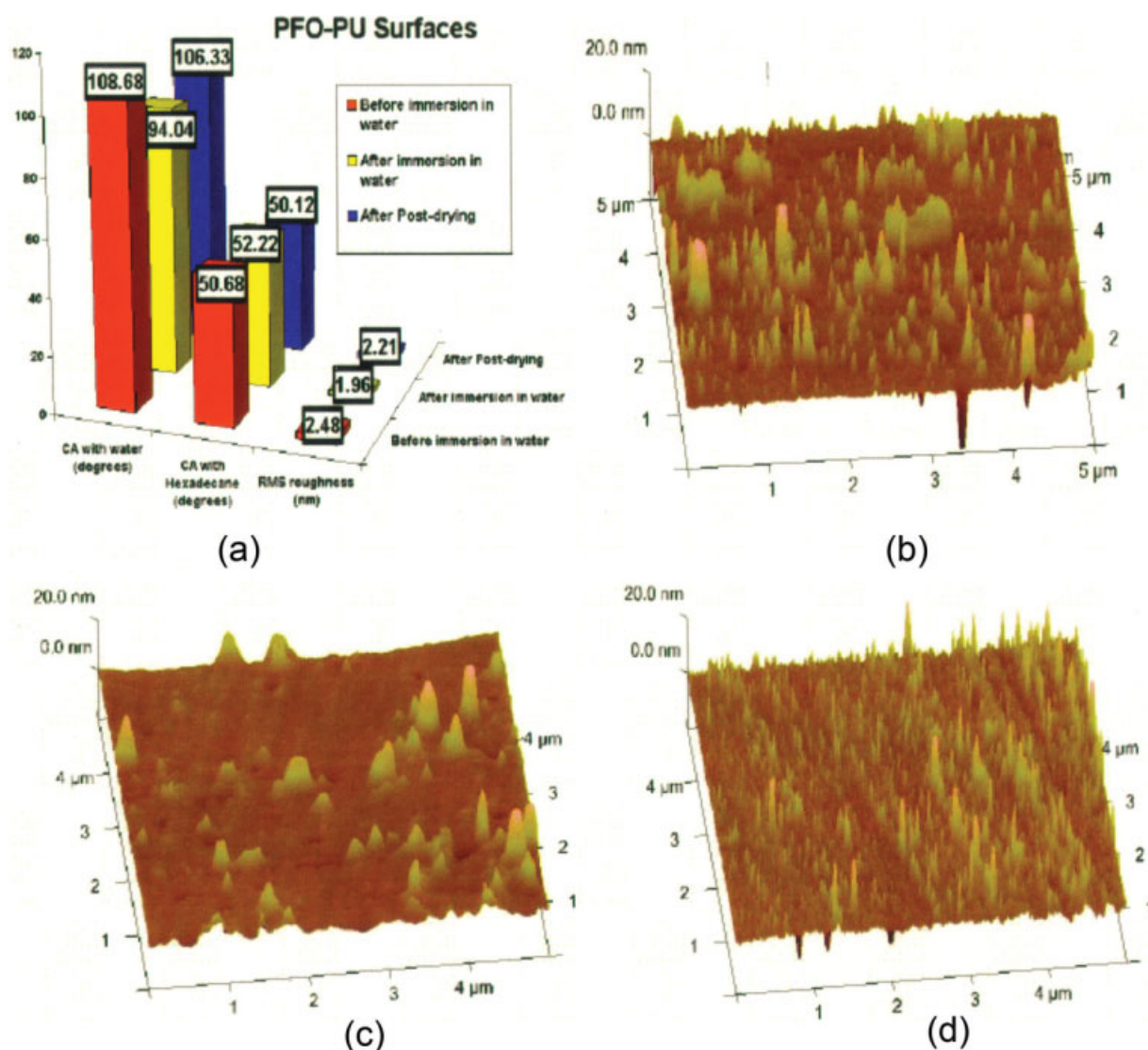
Figure 5 (a) PFO–PU surfaces (CA and rms roughness), (b) AFM image before water immersion, (c) AFM image after water immersion, and (d) AFM image for postdrying. [Color figure can be viewed in the online issue, which is available at www.interscience.wiley.com.]

more organized fashion, thereby increasing the surface roughness and decreasing the surface energy.

Amphiphilic surfaces containing the Zonyl FSO-100 surfactant

The results of the surface analysis of the amphiphilic surfaces under different conditions are shown in Figure 6. Figure 6(a) and the AFM images in Figure 6(b–d) show an interesting behavior of the surfaces containing amphiphilic moieties. These surfaces, like hydrophobic surfaces, became smoother when exposed to water. A decrease in the water CA showed that the surfaces became less hydrophobic in water (compared to air), which may have been because of the orientation of the hydrophobes (perfluoro groups) of the amphiphilic moiety toward the

PU surface. This was thought to result of the greater exposure of the hydrophiles [poly(ethylene oxide) groups] at the surface. An observed increase in the hexadecane CA here was comparable to that for the hydrophilic surfaces. For the postdrying samples, the surface topography changed drastically, and it became more hydrophobic, which was possibly due to a significant increase in the surface roughness and the more uniform reorientation of amphiphilic chains.

Settlement of the *Ulva* zoospores and attachment strength of the sporelings

The poly(ethylene glycol)-modified polyurethane (MRPE) surfaces did not bond strongly to the glass support slides and delaminated, possibly because of the uptake of water and a swelling effect, and could
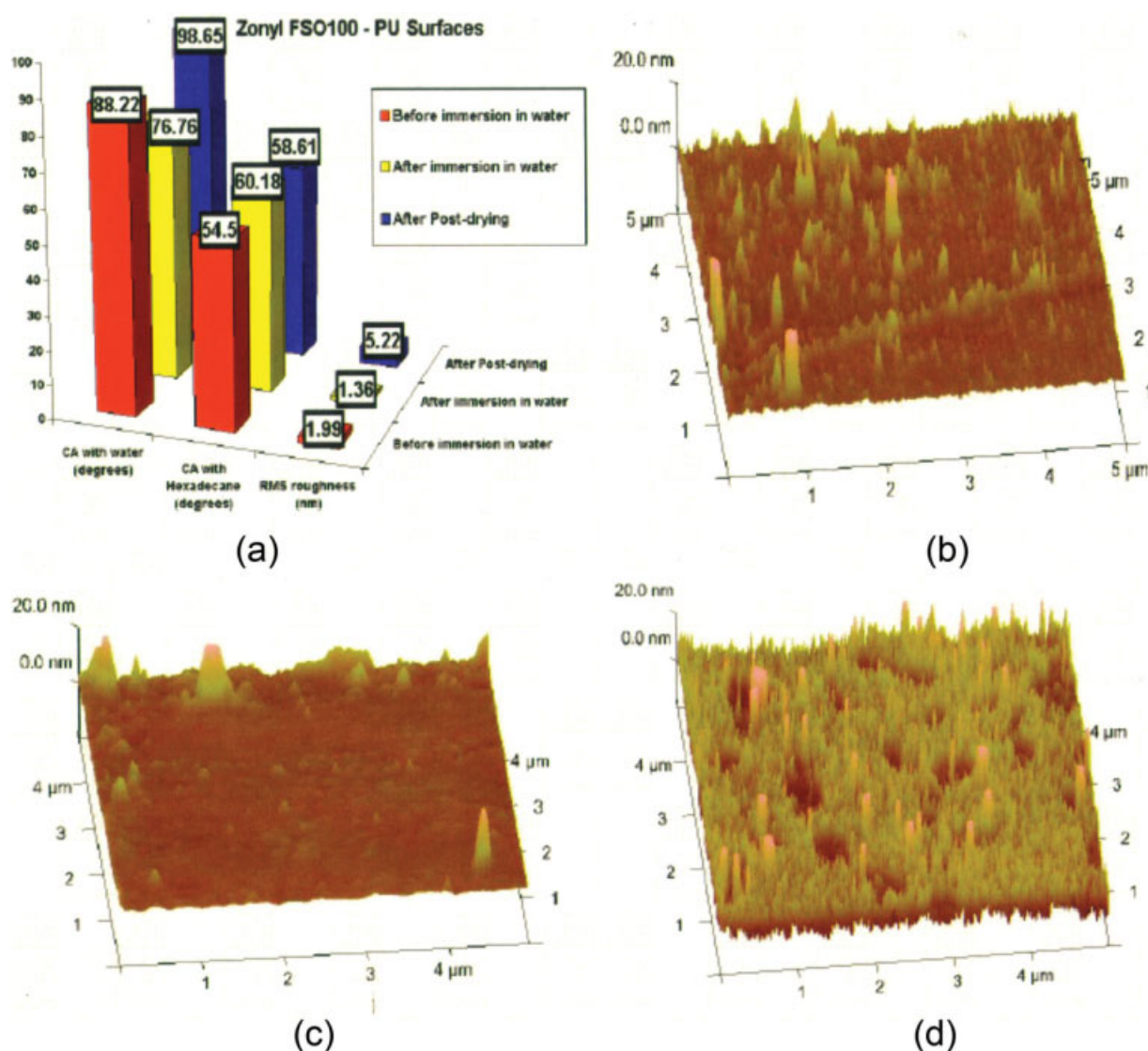
Figure 6 (a) Zonyl FSO-100–PU surfaces (CA and rms roughness), (b) AFM image before water immersion, (c) AFM image after water immersion, and (d) AFM image for postdrying. [Color figure can be viewed in the online issue, which is available at www.interscience.wiley.com.]

not be tested. The inclusion of glass and PDMS surfaces provided nonrelease and foul-release standards, respectively, against which the performance of the urethane samples could be compared.

Spore settlement density was lower on all of the urethane surfaces than on the glass or PDMS standards (Fig. 7). Settlement was lowest on the MRZ100 sample, which was amphiphilic in nature. Spores have been shown previously to settle (attach) in lower numbers on amphiphilic surfaces as compared to glass.[8] The sporelings grew well on all of the surfaces, although there was less biomass on MRZ100, which reflected the low density of settled spores on this surface (Fig. 8). Sporeling attachment strength was weaker on all of the modified urethane surfaces than it was on the PDMS foul-release standard (Fig. 9 and Table II). The high removal indicated
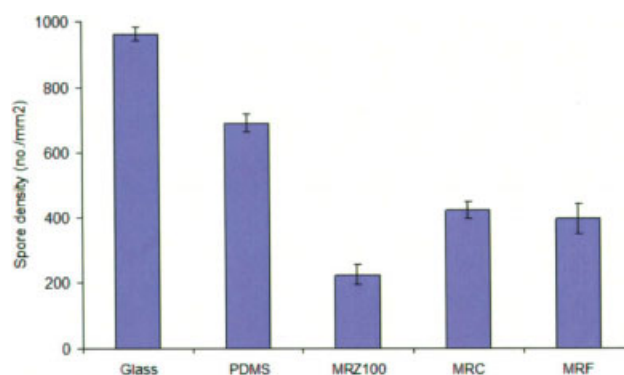

Figure 7 Settlement of the *Ulva* spores on the urethane coatings. The PDMS was T2 Silastic. Each point is the mean of 90 counts (30 from each of the three replicate slides). The bars show the 95% confidence limits. [Color figure can be viewed in the online issue, which is available at www.interscience.wiley.com.]
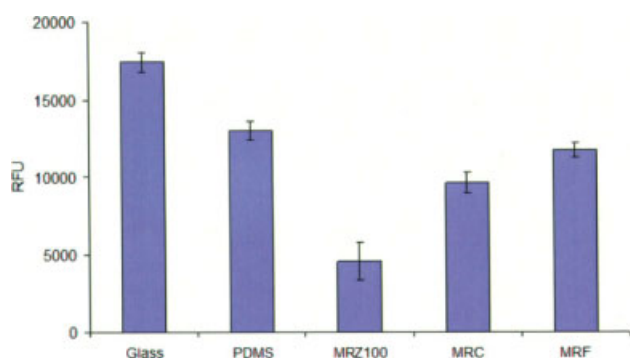
Figure 8 Growth of the *Ulva* sporelings on the urethane coatings after 7 days. Each point is the mean biomass from five replicate slides measured with a fluorescent plate reader. The bars show the standard error of the mean. [Color figure can be viewed in the online issue, which is available at www.interscience.wiley.com.]

that the fluoro and amphiphilic modifications to the basic coating enhanced the release properties. The weakest attachment was on the samples of amphiphilic PU (MRZ100) and hydrophobic PU (MRF). The sporelings were strongly attached to the glass standard.

Plants of the macroalga *Ulva,* in common with other macrofoulers such as barnacles, are well known to adhere weakly to fouling-release coatings based on PDMS.[51] However, the release of macrofouling organisms, including plants of *Ulva,* is less common from coatings based on other types of chemistry. However, weak attachment by the sporelings of *Ulva* has been shown previously for some amphiphilic coatings,[8,52,53] and release from PDMS–PU blends was greater than that from standard PDMS elastomers.[54,55] However, other properties of the MRZ100 and MRF surfaces, including changes in the nanoscale roughness, may also have contributed
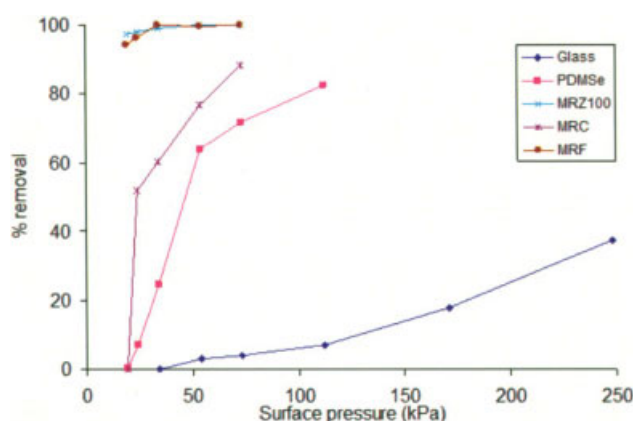
Figure 9 Removal (%) of the 7-day-old sporelings from the urethane coatings plotted as a function of the surface water pressure (kPa). The coatings were exposed to a range of different surface pressures from a water jet. The PDMS was T2 Silastic. [Color figure can be viewed in the online issue, which is available at www.interscience.wiley.com.]

TABLE II
Critical Surface Pressures for 50% Removal of the Sporeling Biofilm

Type	Estimated surface pressure for 50% removal (kPa)
MRZ100	<20
MRF	<20
MRC	25
PDMS	45
Glass	>250

The samples are listed in the order of ease of removal. The data are derived from the curves in Figure 9.

to the weak adhesion strength.[56] The complex restructuring of amphiphilic surfaces underwater is likely to be responsible for the reduced adhesion strength seen for the *Ulva* sporelings.

Overall, both hydrophobic and amphiphilic PU surfaces became somewhat hydrophilic when they were immersed in water. In the former, this behavior was associated with surface topography (decrease in surface roughness); in the later, it was due to the orientation of hydrophilic moieties at the surface. We characterize such dynamic behavior of amphiphilic surfaces as smart because of their capability to respond to the external environment in a predictable manner.

CONCLUSIONS

We report a novel design strategy to fabricate polymeric surfaces with hydrophilic, hydrophobic, and amphiphilic characters. Their dynamic surface characteristics are primarily governed by the chemical composition and surface topography of the films. The study of the dynamic characteristics of such surfaces provided a fundamental understanding of the mechanism underlying their dynamic surface behavior under different external environments. Amphiphilic surfaces resisted biofouling the most among all of the surfaces we studied. Biofouling removal from the amphiphilic and hydrophobic modified surfaces was similar to or better than from the PDMS fouling-release standard. The PU surfaces from tethered dendritic polyol, with their higher strength and tear resistance, offer an attractive alternative to silicones, which are prone to damage. Overall, the amphiphilic PU surfaces with smart surface properties emerged as promising candidates for marine coatings and numerous other potential applications.

References

1. Schultz, M. P. Biofouling 2007, 23, 331.
2. Anderson, C.; Atlar, M.; Callow, M.; Candries, M.; Milne, A.; Townsin, R. L. J Mar Des Operat B 2003, 4, 11.
3. Kiil, S.; Yebra, D. M.; Dam-Johansen, K. Prog Org Coat 2004, 50, 75.
4. Nartensoon, L. Biosci Explained 2005, 2, 1.
5. Jelic-Mrcelic, G.; Sliskovic, M.; Antolic, B. Biofouling 2006, 22, 293.
6. Evans, S. M.; Leksono, T.; McKinnell, P. D. Mar Pollut Bull 1995, 30, 14.
7. Callow, M.; Callow, J. Biologist 2002, 49, 1.
8. Gudipati, C. S.; Finlay, J. A.; Callow, J. A.; Callow, M. E.; Wooley, K. L. Langmuir 2005, 21, 3044.
9. Sweeney, A.; Sanudo-Wilhelmy, S. A. Mar Pollut Bull 2004, 48, 663.
10. Schumacher, J. F.; Aldred, N.; Callow, M. E.; Finlay, J. A.; Callow, J. A.; Clare, A. S.; Brennan, A. B. Biofouling 2007, 23, 307.
11. Schumacher, J. F.; Carman, M. L.; Estes, T. G.; Feinberg, A. W.; Wilson, L. H.; Callow, M. E.; Callow, J. A.; Finlay, J. A.; Brennan, A. B. Biofouling 2007, 23, 55.
12. Genzer, J. A.; Efimenko, K. Biofouling 2006, 22, 339.
13. Adkins, J.; Mera, A.; Roe-Short, M. A.; Pawlikowski, G. T.; Brady, R. F. Prog Org Coat 1996, 29, 1.
14. Anastasiadis, S. H.; Restos, H.; Pispas, S.; Hadjichristidis, N. Macromolecules 2003, 36, 1994.
15. Chaudhury, M. K.; Thanawala, S. K. Langmuir 2000, 16, 1256.
16. Chaudhury, M. K.; Vaidya, A. J Colloid Interface Sci 2002, 249, 235.
17. Cunliffe, D.; Smart, C. A.; Alexander, C.; Vulfson, E. Appl Environ Microbiol 1999, 65, 4995.
18. Gilcreest, V. P.; Carroll, W. M.; Rochev, Y. A.; Blute, I.; Dawson, K. A.; Gorelov, A. V. Langmuir 2004, 20, 10138.
19. Halabieh, R.; Mermut, O.; Barrett, C. Pure Appl Chem 2004, 76, 1445.
20. Houbenov, N.; Minko, S.; Stamm, M. Macromol Commun 2003, 36, 5897.
21. Jin, L.; Young, M. J.; Lee, W. K.; Park, D. K.; Young, K. H. J Biomed Mater Res 1998, 40, 314.
22. Kohl, J. G.; Singer, I. L. Prog Org Coat 1999, 36, 15.
23. Leonid, I.; Nikolay, H.; Sidorenko, A.; Manfred Stamm, M. Langmuir 2004, 20, 9916.
24. Lundberg, D. J.; Brown, R. G.; Glass, J. E.; Eley, R. R. Langmuir 1994, 10, 3027.
25. Minko, S.; Usov, D.; Goreshnik, E.; Stamm, M. Macromol Rapid Commun 2001, 22, 206.
26. Ober, C. K.; Youngblood, J. P.; Hexemer, A.; Callow, M. E. Biofouling 2003, 19, 91.
27. Roosjen, A.; Vries, J.; van der Mei, H. C.; Norde, W.; Busscher, H. J. J Biomed Mater Res B 2005, 73, 347.
28. Taolei, S.; Guojie, W.; Lin, F.; Liu, B.; Ma, Y.; Lei, J.; Zhu, D. Angew Chem Int Ed 2004, 43, 357.
29. Wang, Y.; Zheng, J.; Brittain, W. J.; Cheng, S. J Polym Sci Part A: Polym Chem 2006, 44, 5608.
30. Yong, P.; Jing, M. J Am Chem Soc 2005, 127, 6802.
31. Zhiguang, G.; Feng, Z.; Jingcheng, H.; Weimin, L. Am Chem Soc Commun 2005, 127, 15670.
32. Katsikogianni, M.; Missirlis, Y. F. Eur Cells Mater 2004, 8, 37.
33. Yuehuei, H.; Friedman, R. J. J Biomed Mater Res Appl Biomater 1998, 43, 338.
34. Callow, J. A.; Callow, M. E. In Biological Adhesives; Smith, A. M.; Callow, J. A. E., Eds.; Springer-Verlag: Berlin, 2006.
35. Goel, A.; Joshi, R. G.; Mannari, V. J Coat Technol Res 2009, 6, 123.
36. Joshi, R. G.; Goel, A.; Mannari, V. In Smart Coatings 2007 Conference Proceedings; Baghadachi, J.; Provder, T., Eds.; American Chemical Society: Washington, DC, 2007.
37. Joshi, R. G.; Goel, A.; Mannari, V.; Finlay, J. A.; Callow, M.; Callow, J. A. In American Coatings 2008 Conference Proceedings; Vincentz Network: Charlotte, NC, 2008.
38. Statz, A.; Finlay, J.; Dalsin, J.; Callow, M.; Callow, J. A.; Messersmith, P. B. Biofouling 2006, 22, 391.
39. Wouters, M.; Zanten, J. V.; Hujis, F.; Vereijken, T. JCT Res 2005, 1, 435.
40. Brady, R. F. J. Prog Org Coat 1999, 35, 31.
41. Brady, R. F., Jr. Composition and Performance of Fouling Release Coatings. In Assessing the Future of Coating Work, Proceedings of the PCE 2000 Conference and Exhibition; Genoa, Italy, 2006, p 7.
42. Callow, M. E.; Callow, J. A.; Pickett-Heaps, J. D.; Wetherbee, R. J Phycol 1997, 33, 938.
43. Chaudhury, M. K.; Finlay, J. A.; Chung, J. Y.; Callow, M. E.; Callow, J. A. Biofouling 2005, 21, 41.
44. Schultz, M. P.; Finlay, J. A.; Callow, M. E.; Callow, J. A. Biofouling 2003, 19, 17.
45. Boltorn® Technical Information Brochure: Boltorn® H2004; Perstorp Specialty Chemicals: Perstorp, Sweden, 2009; p 7.
46. Götz, H.; Beginn, U.; Bartelink, C. F.; Grünbauer, H. J. M.; Möller, M. Macromol Mater Eng 2002, 287, 223.
47. Cassé, F.; Stafslien, S. J.; Bahr, J. A.; Daniels, J.; Finlay, J. A.; Callow, J. A.; Callow, M. E. Biofouling 2007, 23, 121.
48. Finlay, J. A.; Callow, M. E.; Schultz, M. P.; Swain, G. W.; Callow, J. A. Biofouling 2002, 18, 251.
49. Koberstein, J. T. J Polym Sci Part B: Polym Phys 2004, 42, 2942.
50. Kober, M.; Wesslén, B. J Appl Polym Sci 1994, 54, 793.
51. Beigbeder, A.; Degee, P.; Conlan, S.; Mutton, R.; Clare, A. S.; Pettitt, M. E.; Callow, M. E.; Callow, J. A.; Dubois, P. Biofouling 2008, 24, 291.
52. Krishnan, S.; Ayothi, R.; Hexemer, A.; Finlay, J. A.; Sohn, K. E.; Perry, R.; Ober, C. K.; Kramer, E. J.; Callow, M. E.; Callow, J. A.; Fischer, D. A. Langmuir 2006, 22, 5075.
53. Martinelli, E.; Agostini, S.; Galli, G.; Chiellini, E.; Glisenti, A.; Pettitt, M. E.; Callow, M. E.; Callow, J. A.; Graf, K.; Bartels, F. W. Langmuir 2008, 24, 13138.
54. Cassé, F.; Ribeiro, E.; Ekin, A.; Webster, D. C.; Callow, J. A.; Callow, M. E. Biofouling 2007, 23, 267.
55. Ekin, A.; Webster, D. C.; Daniels, J. W.; Stafslien, S. J.; Cassé, F.; Callow, J. A.; Callow, M. E. J Coat Technol Res 2007, 4, 435.
56. Majumdar, P.; Lee, E.; Patel, N.; Ward, K.; Stafslien, S. J.; Daniels, J.; Boudjouk, P.; Callow, M. E.; Callow, J. A.; Thompson, S. E. M. Biofouling 2008, 24, 185.